

Selective Activation of C=C Bond in Sustainable Phenolic Compounds from Lignin *via* Photooxidation: Experiment and Density Functional Theory Calculations

Morgan Zielinski (Goldberg), Luke A. Burke and Alexander Samokhvalov*

Chemistry Department, Rutgers University, Camden, NJ

Received 9 June 2015, accepted 4 August 2015, DOI: 10.1111/php.12509

ABSTRACT

Lignocellulosic biomass can be converted to high-value phenolic compounds, such as food additives, antioxidants, fragrances and fine chemicals. We investigated photochemical and heterogeneous photocatalytic oxidation of two isomeric phenolic compounds from lignin, isoeugenol and eugenol, in several nonprotic solvents, for the first time by experiment and the density functional theory (DFT) calculations. Photooxidation was conducted under ambient conditions using air, near-UV light and commercial P25 TiO₂ photocatalyst, and the products were determined by TLC, UV–Vis absorption spectroscopy, HPLC–UV and HPLC–MS. Photochemical and photocatalytic oxidation of isoeugenol proceeds *via* the mild oxidative “dimerization” to produce the lignan dehydrodiisoeugenol (DHDIE), while photooxidation of eugenol does not proceed. The DFT calculations suggest a radical stepwise mechanism for the oxidative “dimerization” of isoeugenol to DHDIE as was calculated for the first time.

INTRODUCTION

Biomass is thought to partially replace fossils in production of “green” chemicals (1–3)—the small organic molecules from biomass, *e.g.* monomers for the synthesis of sustainable bioinspired polymers (4–6). According to the U.S. Biobased Industry Targets, >90% of organic chemicals can be produced by 2090 from biomass and “platform chemicals” obtained from biomass (7). Lignin is the second major (after cellulose) component of wood, and is a biopolymer of a very complex structure (8); the simplified formula of its tentative “monomer” is explained in Fig. 1a.

In Fig. 1a, the R₁ and R₂ indicate the short oxygen-containing chains with alkyl, olefin or substituted aryl groups. The “bio-oil” produced *via* depolymerization of lignin (9) at the LignoCellulose Feedstock Biorefinery (7) contains the high concentrations of valuable organic compounds. Phenolic compounds from lignin (10) belong to the “lignin platform” and hold an especially high promise for synthesis of sustainable chemicals. The following oxidation reactions of phenolic compounds from lignin are known: 1) chemical oxidation (11); 2) heterogeneous catalytic oxidation (12); 3) photochemical oxidation with photosensitizer dye (13) and 4) heterogeneous photocatalytic oxidation (14).

Chemical oxidation relies upon expensive and/or toxic chemicals, while catalytic oxidation uses elevated temperatures and expensive catalysts, *e.g.* Pt group metals (15). Photochemistry and photocatalysis can be regarded as methods of “Green Chemistry” (16), since they proceed under ambient temperature and pressure, and use air and sunlight (17).

Isoeugenol (Fig. 1b) is one of the most abundant (up to 7%) chemical components in bio-oil (7). Isoeugenol and eugenol (Fig. 1c) are used as fragrances (13) and antioxidants (18). Oxidation of eugenols produces lignans (19) including dehydrodiisoeugenol (DHDIE) (20). DHDIE is used as a natural medicine compound with anti-inflammatory (21) properties similar to those of the nonsteroidal anti-inflammatory drugs, and selective enzyme inhibiting properties (22). Synthetic medicinal drugs in river water (23) and drinking water (24) pose a significant health concern worldwide. Unlike certain recalcitrant synthetic drugs, especially estrogen mimics (25) and endocrine disrupting phthalates (26), bioactive phenolic compounds from lignin can be easily removed from wastewater *via* photocatalytic mineralization under ambient conditions and sunlight (14).

Photooxidation of isoeugenol with photosensitizer proflavin dihydrochloride in methanol leads to several products (27) of oxidative “dimerization”: DHDIE and two β -aryl ethers. Photosensitized oxidation of isoeugenol with methylene blue (MB) gives seven products in methanol, seven in ethanol, six in acetone and five in acetonitrile (18). Photosensitized oxidation of isoeugenol with MB dye in water/CH₃CN produces several dimeric cyclic or acyclic lignans (28). Photosensitized oxidation of eugenol by Rose Bengal dye or chlorophyll leads to the products of quinoid structure (13), thus photosensitized oxidation is nonselective *vs* functional groups: phenyl ring, C=C bond and OH group. In all reported studies of photooxidation of eugenols, organic photosensitizer was used and several reaction products were obtained. Organic photosensitizer is difficult to remove from reaction mixture after the reaction is completed, and it can undergo photodecomposition. Photooxidation of eugenols in solution in the nonprotic solvents without organic photosensitizer dye has not been investigated, to the best of our knowledge.

The density functional theory (DFT) is an *ab initio* technique of quantum chemistry that is commonly used to study the mechanisms of chemical reactions of organic compounds by calculation of the energies and geometries of transition states (TSs) and intermediates (INT) (29). The structure–activity relationships in the antioxidant effects of several phenolic compounds from lignin were investigated by the DFT (30). The antioxidant activity

*Corresponding author email: alexsam@camden.rutgers.edu (Alexander Samokhvalov)

© 2015 The American Society of Photobiology

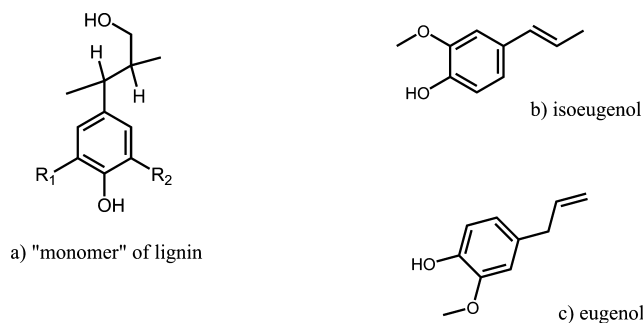


Figure 1. Molecular structures of (a) tentative “monomer” of lignin; (b) isoeugenol; (c) eugenol.

has been assigned to the combination of the heat of formation of the radical and spin delocalization (30), while TSs leading to reactive INT were not considered. To the best of our knowledge, studies of the mechanism of oxidation of isoeugenol have not been reported by the DFT calculations.

Heterogeneous photocatalysis occurs after absorption of the photon by the photocatalyst. Photocatalytic reactions proceed under the “green” ambient conditions (31) and utilize the abundant, free, environmentally clean and virtually unlimited sunlight or its near-UV fraction (32). Titanium dioxide TiO_2 Degussa P25 recently rebranded as Evonik Aeroxide (31) is a benchmark photocatalyst with a high stability and activity in the UV range. Titanium dioxide is among the 50 most used chemicals in the world (33), but the only report on using TiO_2 in photocatalytic reactions of eugenols is a complete oxidation of eugenol in waste waters (34) to carbon dioxide and water. Heterogeneous photocatalytic oxidation of phenolic compounds from lignin in solution in the nonprotic solvents to organic compounds has not been reported, to the best of our knowledge.

Recently, we reported the synthesis, structural and spectroscopic characterization, and testing of the novel titanium oxide based photocatalysts (35) and sorbents (36) that operate in solution under ambient conditions. Herein, we report the study of the selectivity of photochemical and photocatalytic oxidation of major phenolic compounds from lignin, isoeugenol and eugenol, in several nonprotic solvents at 30°C , $\lambda_{\text{exc}} \geq 300$ nm, with ambient air at 1 atm, with and without P25 TiO_2 . We also report, for the first time, the DFT calculations of the mechanism of oxidative “dimerization” of isoeugenol.

MATERIALS AND METHODS

Chemicals. Eugenol, isoeugenol and vanillin were from Sigma Aldrich, and were used as received. Acetonitrile CH_3CN , dimethylformamide (DMF) and dimethylsulfoxide (DMSO) with an assay $>99.7\%$ were from Sigma, Fisher and Acros Organics and were used as received. Titanium dioxide P25 Evonik Aeroxide was from Acros Organics.

Photoreactor. The custom-built photoreactor contained a light source and reaction vessel (RV) placed inside the liquid circulation thermostat, Neslab model EX221 filled with the mixture of water and ethylene glycol, and operated at 30°C . The light source was a commercial 450 W medium pressure quartz mercury vapor lamp from Ace Glass (37). The RV made of Pyrex transmits light with $\lambda \geq 300$ nm, while the infrared radiation emitted by the mercury lamp is absorbed by the thermostat carrier fluid. The size of RV was 200 mm in length and 32 mm in diameter, and it received humidified ambient air (*ca* 90% relative humidity) as oxidant.

Photooxidation in the absence of photocatalyst. Ten milliliter of the 0.5 M solution of the chosen phenolic compound in a chosen solvent was

placed into the RV and allowed to react for 4 h in the flow of air at 25 mL min^{-1} ; in the experiments without solvent, 10 g pure eugenol or isoeugenol was used.

Product analysis. TLC was used to identify products of chemical reactions using silica gel plates from Sigma Aldrich and a 60/40 mixture of hexane/ethyl acetate as an eluent, with UV visualization (38). UV-visible spectroscopy (UV-Vis) was applied to assess the progress of photooxidation reactions, using the Cary Bio-Rad 50 spectrometer in absorbance mode. Usually, $3 \mu\text{L}$ of a clear supernatant were diluted with acetonitrile up to 3 mL, and a quartz cuvette with $l = 1$ cm was used. For the HPLC with the UV-Vis and mass spectrometric (MS) detection using an electrospray ionization (HPLC-UV-MS-ESI), the 6410 Triple Quad LC/MS 1200 Series instrument from Agilent was used. A C18 reverse phase column with stationary phase at $3.5 \mu\text{m}$ in diameter was used. Samples of reaction products were volumetrically diluted by a factor of 1000 prior to injection into the HPLC-UV-MS-ESI instrument. The mobile phase in the HPLC was a mixture of 0.1 vol. % formic acid in water and 0.1 vol. % formic acid in CH_3CN , and a gradient elution was used; for each specimen, at least three replicas were obtained.

Reference compound. The reference compound DHDIE was synthesized and purified following the modified procedure (39). Briefly, a solution of 70 g FeCl_3 in 200 mL water was added drop-wise to a solution of 50 g isoeugenol in 450 mL ethyl alcohol and 200 mL water, until the solution turned dark green and cloudy. The original synthesis (39) required a few crystals of DHDIE to initiate crystallization; instead, the solution was kept in the freezer for 1 week, and it produced a reddish white crystalline precipitate in a dark yellow solution. The crystals were isolated *via* vacuum filtration, washed with hexane and recrystallized from hot hexane. The chemical identity of the DHDIE obtained was established by melting point (39) using a Mel-Temp apparatus, retention time on the HPLC-UV chromatogram, and the mass spectra in the HPLC-UV-MS as reported elsewhere (40).

Quantum chemical calculations. All calculations were carried out with the Gaussian09 suite of computer programs (41) using its standard threshold and defaults. The DFT theoretical method was employed using the unrestricted PBE0 functional (42,43), $6 - 1 + \text{G(d)}$ basis set, and analytical gradients.

Photocatalytic oxidation. Photocatalytic oxidation was conducted under the conditions similar to those of the photochemical oxidation (above), except that 50 mg of TiO_2 was added. After reaction, the samples of suspension containing TiO_2 were centrifuged at $16\,060 \times g$ (Fisher Scientific AccuSpin Micro). The supernatant was analyzed by the TLC, UV-Vis, HPLC-UV and HPLC-MS-ESI methods as described above.

RESULTS

Photochemical oxidation of eugenol and isoeugenol

Photochemical oxidation experiments were conducted in a Pyrex RV, with the spectrum of transmitted light as in Fig. 2. This is a strong emission line at $\lambda = 313$ nm (marked with an asterisk *) that would cause the photoexcitation of the molecules of eugenol and isoeugenol which have absorption bands at *ca* 310–325 nm, as determined by the UV-Vis spectroscopy in solution (data not shown).

Acetonitrile CH_3CN has initially been chosen as solvent, since it 1) has a high solubility of oxygen under standard conditions (44); 2) is optically transparent for the excitation light used by us and 3) is a “yellow” solvent by the scale of being environmentally and toxicologically “green” (45). We have found by TLC that isoeugenol, but not eugenol, formed products of photooxidation when dissolved in acetonitrile. Furthermore, in the UV-Vis absorption spectrum of the solution of isoeugenol but not eugenol, there was a change in the relative amplitude/area of absorption peaks at 240–280 vs 310–325 nm before and after photooxidation. Thus, isoeugenol undergoes photochemical oxidation in solution, while eugenol does not. In the reference

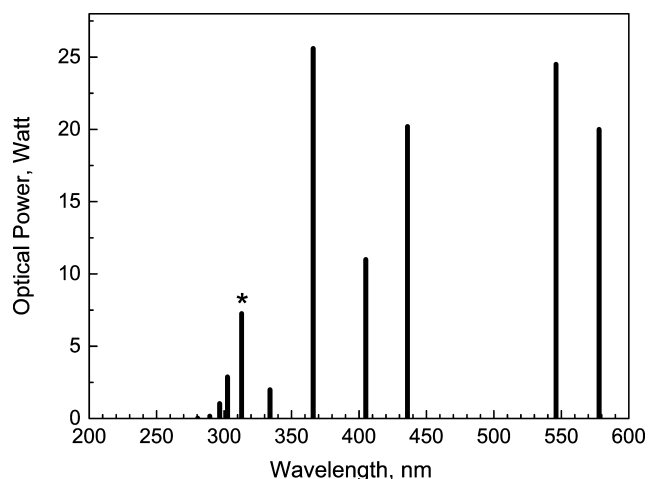


Figure 2. The spectrum of the light used in the photooxidation of phenolic compounds from lignin in solution. The * mark indicates emission line which corresponds to optical absorption band of isoeugenol and eugenol in solution.

experiments in the dark, no products of oxidation of isoeugenol or eugenol have been detected, as expected.

We have used the HPLC-UV method to identify and quantify the products of the photooxidation of isoeugenol at $\lambda_{\text{abs}} = 275$ nm which corresponds to the absorption maximum of isoeugenol in solution. The HPLC-UV chromatogram of the solution of pure isoeugenol shows one peak as expected, at the retention time 10.0 min. Under photochemical oxidation, isoeugenol reacts in solution to form two products as found by the HPLC-UV-MS. One product is vanillin with retention time 8.8 min as identified by injection of the vanillin standard. Another product results in the HPLC-UV peak at retention time 11.0 min. We have checked a hypothesis that this product is DHDIE, by comparing its HPLC-UV retention time and the mass spectrum with those of the DHDIE standard synthesized and purified by us (see Materials and Methods). The mass spectrum of DHDIE has three characteristic peaks at $m/z = 327$, 349, and 675 a.m.u. (40). Assignments of those peaks are as follows: $[M + H]^+$ for 327 a.m.u., $[M + Na]^+$ for 349 a.m.u. and $[2M + Na]^+$ for 675 a.m.u., with M being the molecule of DHDIE; the MS peaks are consistent with those reported (40) for DHDIE.

Without solvent, isoeugenol produced only the small amounts of DHDIE, and eugenol did not yield any products. We have selected several nonprotic solvents other than CH_3CN for the photooxidation in solution. Dimethylsulfoxide has a high dipole moment of 4.3 D (46) and is a “yellow” solvent by the scale of “being green” (45). Dimethylformamide was also tested by us, since it has a high dipole moment of 3.86 D. We checked the possibility of the photooxidation of each solvent. First, all solvents have absorption peaks only at $\lambda < 260$ nm and therefore their molecules, unlike the molecules of isoeugenol or eugenol, do not absorb the near-UV light. Second, we have conducted the reference HPLC-UV analysis of reaction mixtures, with optical detection at the multiple wavelengths: $\lambda_{\text{abs}} = 220$, 254 and 275 nm, and did not find any peaks due to chemical substances other than eugenol, isoeugenol, DHDIE and vanillin. Third, we have checked the three solvents used after a “blank” experiment of photooxidation without dissolved substrate by the HPLC-UV-

MS analysis, and did not find any peaks due to the products of oxidation or photolysis. Therefore, the solvents acetonitrile, DMF and DMSO are stable under the conditions of photochemical oxidation.

Figure 3 shows the reaction network of photochemical oxidation of isoeugenol.

The lignan DHDIE is more valuable than vanillin, since the former is a product of synthesis, rather than destruction of the reactant molecule, so we decided to investigate the dependence of the molar concentration of DHDIE product on the choice of the nonprotic solvent. We determined molar concentrations of the DHDIE product by the HPLC-UV method (47). Figure 4 shows the HPLC-UV calibration plot obtained with the DHDIE standard at $\lambda_{\text{abs}} = 275$ nm.

As an injected volume of the solution of DHDIE has been increased, there was a corresponding linear increase in the absorbance at 275 nm. The HPLC-UV calibration plot in Fig. 4 was used to determine the molar concentrations of DHDIE obtained in photochemical oxidation of isoeugenol. Figure 5a shows the dependence of the molar concentration of the DHDIE product (in mM) on the dipole moment of each solvent used in the photochemical oxidation.

Although DMSO, DMF and CH_3CN have very close values of the dipole moment, they produced the significantly different amounts of DHDIE. Figure 5b shows the dependence of the

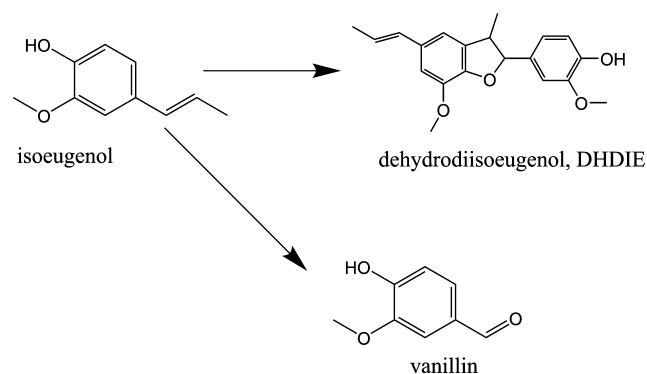


Figure 3. Reaction network of the photochemical and photocatalytic oxidation of isoeugenol in solution.

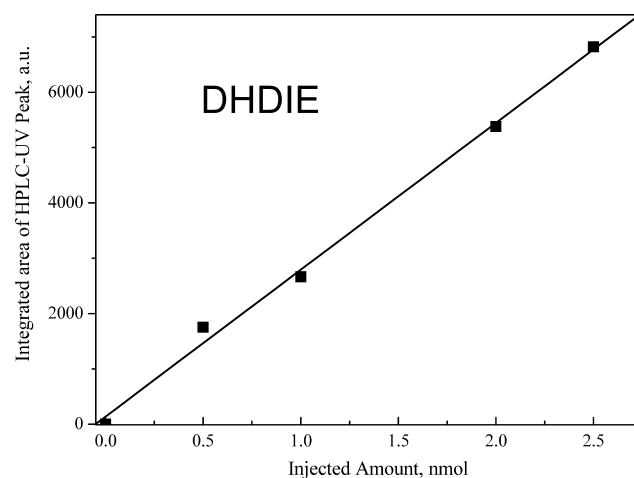


Figure 4. The HPLC-UV calibration plot of dehydrodiisoeugenol (DHDIE) in solution at $\lambda = 275$ nm.

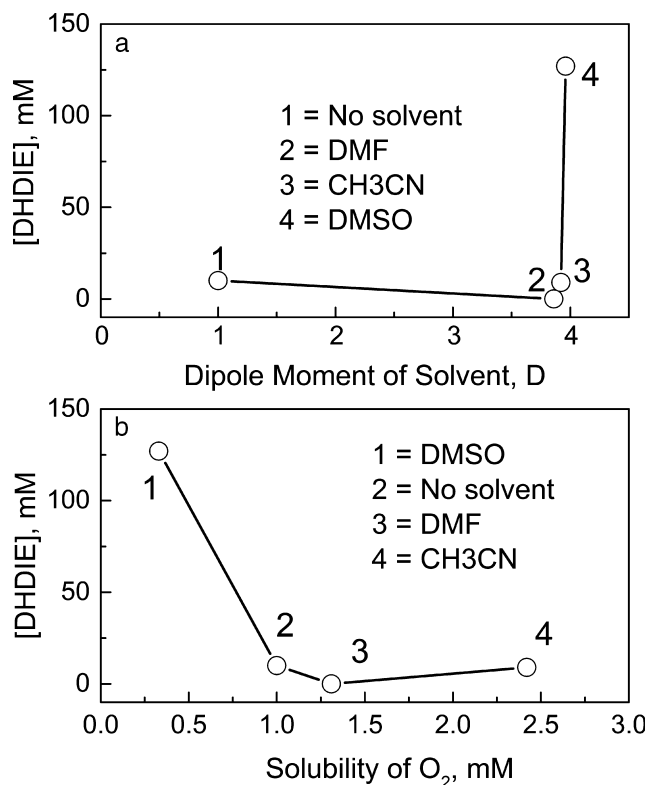


Figure 5. Molar concentration of the dehydrodiisoeugenol (DHDIE) product in the photochemical oxidation in solution: (a) vs the dipole moment of the solvent; (b) vs oxygen solubility in the solvent.

molar concentration of the DHDIE product on the solubility of oxygen (44,48) in each solvent. The DMF (1.31 mM dissolved O₂) and CH₃CN (2.42 mM O₂) have the higher oxygen solubility than DMSO, yet they yield the lower concentrations of DHDIE compared to DMSO. Therefore, the much higher yield of the DHDIE obtained in DMSO vs other solvents is due to some property of DMSO. Both the radical and radical cation of isoeugenol were generated in the solution of isoeugenol (49) by photolysis at 308 nm which is close to $\lambda = 313$ nm, the excitation wavelength in our reactions, Fig. 2. Radical cation of isoeugenol undergoes a quick loss of proton to yield the more stable radical isoeugenol (49) (Scheme 1).

The DMSO is an electron donor that strongly solvates cations (46); it is therefore speculated that DMSO solvates a radical cation of isoeugenol (49) and accelerates the rate of formation of DHDIE as the only “dimeric” product. On the other hand, reported mild chemical oxidation of isoeugenol by stable radical DPPH in methanol yields a complex mixture of DHDIE and its methylated derivatives (40).

In our photooxidation tests, isoeugenol underwent oxidative “dimerization,” while eugenol did not react. Contrary to that, both isoeugenol and eugenol underwent “mild” chemical oxidation (40) yielding the mixture of several lignans including dehydrodieugenol (product of oxidation of eugenol) and its methylated derivatives. Thus, photochemical oxidation in DMSO as reported by us has the following advantages vs reported “mild” chemical oxidation (40): 1) photochemical oxidation selectively proceeds via internal C=C bond in isoeugenol, but not terminal C=C bond in eugenol and 2) photochemical oxidation leads to fewer number of products. To the best of our

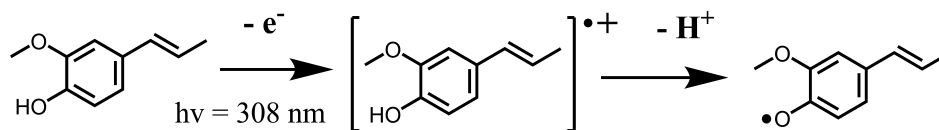
knowledge, the mechanism of oxidation of isoeugenol has not been studied by the methods of quantum chemistry. We have applied the DFT method to study the mechanism of reaction of isoeugenol to form DHDIE.

Reaction of isoeugenol by the DFT calculations

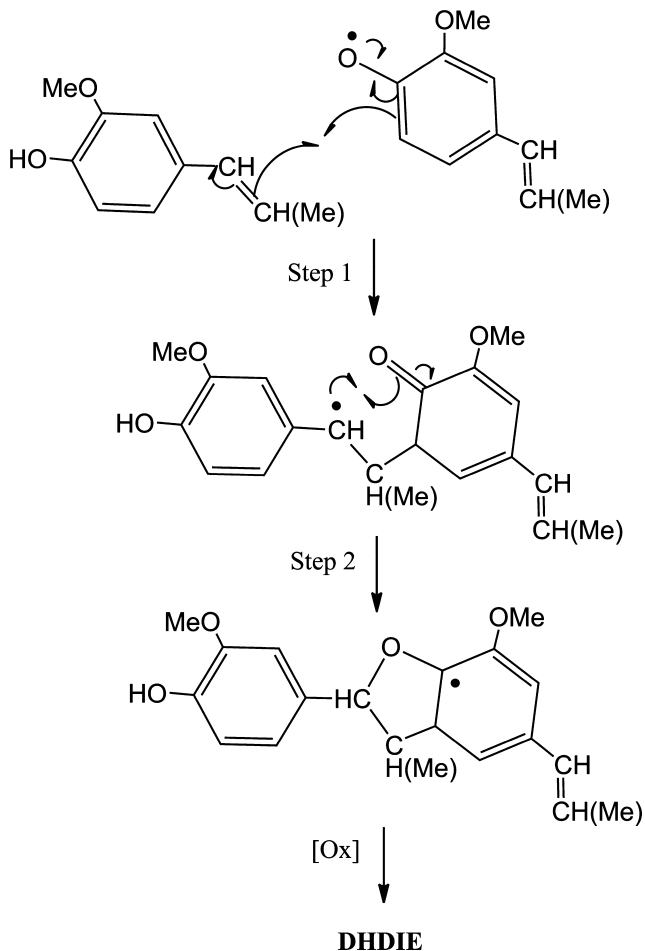
A DFT computational experiment was undertaken to elucidate the possible mechanisms for the dimerization of isoeugenol, in particular, to calculate the pathways to the neutral radical–neutral molecule product, including TSs and INT in the formation of the cyclic dimeric product. It is assumed that this intermediate cycloaddition product then undergoes facile loss of hydrogen to give the final, conjugated product (DHDIE). All calculations were carried out with the Gaussian09 suite of computer programs (41) using its standard threshold and defaults. The DFT theoretical method was employed using the unrestricted PBE0 functional (42,43), 6 – 31 + G(d) basis set, and analytical gradients. The PBE0 functional (Gaussian09 keyword PBE1PBE) has been shown to be effective in radical and excited state calculations (50). The 6 – 31 + G(d) basis set is considered an effective basis set for both excited state and cycloaddition reactions since it contains diffuse functions needed in TSs and radical reactions (51). All critical points were examined for the proper number of imaginary frequencies, and the vectors for the imaginary frequency in each TS structure followed the motions expected for bond breaking/formation or rotation. In our DFT model, we assumed that the “dimerization” of isoeugenol starts with the abstraction of a hydroxyl hydrogen atom from the molecule of isoeugenol. Scheme 2 gives the sequence of the neutral radical and a molecule of isoeugenol combining to form a benzylic radical intermediate (step 1), and then the benzylic radical and carbonyl combining to form a dimer-like cyclic product (step 2).

Two starting structures in the optimization procedure for step 1 were tested using the cycloaddition dimer as a framework: one resembling the concerted mechanism whereby the ringC–CH(Me) and HC–O bonds were each elongated to 2.0 Å and the other involving a two-step mechanism obtained by slightly elongating the new ringC–CH(Me) bond in the dimer to 1.6 Å, but increasing the former HC–O bond to ca 3 Å. The TS optimization procedure for the concerted starting structure continued to the identical TS structure as the first step in a two-step mechanism. The activation energy, E_a (kcal mol⁻¹) of bond breaking is calculated as the difference in energy of the first step TS and a van der Waals structure found for the two reactants, thus avoiding basis set superposition error and concentrating on relative energies of any TS structure or INT. The intermediate and two TS expected for a two-step mechanism were found. However, there are at least two approaches in the first step which form rotameric isomers of the radical intermediate, wherein the C–CHAr bond is at a dihedral angle of either *gauche* 60° or *anti* 180° to the C–H bond at the site of attachment on the keto ring. (The *gauche* is pictured in Scheme 2.) Here, the benzylic radical centers are planar sp² and the two carbons forming the new bond are each pyramidalized toward an sp³ center, as can be seen in the DFT-optimized structures in the Supporting Information, *vide infra*.

When the *gauche* and *anti* benzylic radical approaches were considered, seven structures were found for the neutral radical–neutral molecule dimerization reaction. The first structure is a van der Waals complex of the reactants in a position resembling the *anti* TS (TS1) (second structure) for the formation of the



Scheme 1. Formation of the radical cation and radical of isoeugenol from isoeugenol under the near-UV light.



Scheme 2. Stage-wise reaction of the radical of isoeugenol with a molecule of isoeugenol through radical intermediates.

third structure which is the *anti* 180° intermediate (Int1). This *anti* structure can then rotate through an eclipsed rotational TSr (fourth structure) to form the *gauche* 60° intermediate (Int2) (fifth structure). The *gauche* intermediate then goes through a TS structure (TS CO) (sixth structure, center structure of Scheme 2) which then forms the ring product (seventh structure).

The DFT-optimized structures are provided in the Supporting Information: van der Waals reactants (Figure S1), TSs Int1 (Figure S2), TSr (Figure S3), Int2 (Figure S4), TS CO (Figure S5) and the cycloproduct (Figure S6); TS TS1 looks very similar to Int1 and is not shown. An energetically unfavorable TS2 (*gauche*) state is provided in Figure S7. The Cartesian coordinates and Gaussian09 input files of the DFT-optimized reactants, TSs TS1, Int1, TSr, Int2, TS CO, the cycloproduct and intermediate TS2 are provided in the Table S1. It was found that the TS for the formation of the *anti* 180° intermediate is *ca* 2 kcal mol⁻¹ lower than the TS for the formation of the *gauche* 60° intermediate (TS2). The formation of the C–O

bond is the rate limiting step and the formations of the radical intermediate through the *gauche* and *anti* rotamers (Scheme 2) are competitive to each other. Figure 6 shows the calculated reaction profile.

The spin density on the reactants and product lies on the *keto* ring fragment, while the spin density of the INT is localized in the conjugated –CHAr fragment. This might account for the absence of cyclic product with eugenol rather than isoeugenol. The unpaired electron in the radical intermediate with the eugenol isomer, if it could be formed, would not have resonance stabilization with the Ar group due to the intervening CH₂ group in the –CHCH₂Ar fragment. Table 1 provides the total energies in Hartrees and energies in kcal mol⁻¹ relative to the van der Waals complex of the reactants. Also given is the energy and relative energy for the TS2 leading directly to Int2 from the van der Waals complex *via* the *gauche* approach.

After finding the reaction mechanism involving a neutral radical, the search for a similar pathway was attempted for the dimerization of two neutral molecules, *i.e.* without involving a hydrogen abstraction, but no TS structure could be found for the dimerization of two neutral molecules. After the DFT computational study of photooxidation of eugenol and isoeugenol, we proceeded to experimental work on photocatalytic oxidation in the presence of titanium dioxide in solution.

Photocatalytic oxidation of eugenol and isoeugenol with P25 TiO₂

To the best of our knowledge, photocatalytic oxidation of eugenols in the nonprotic solvents has not been reported. Titanium dioxide TiO₂ Degussa P25 recently rebranded as Evonik Aeroxide (31) is a benchmark photocatalyst which consists of *ca* 80% anatase, rutile and some amorphous phase (52) and has the total surface area of 30–50 m² g⁻¹. We have chosen to use 50 mg TiO₂ photocatalyst per 10 mL liquid phase (see Materials and Methods), since such a solid/liquid ratio is close to the high limit of the range 0.5–3.0 g L⁻¹ recommended in the recent critical note (53) for the photocatalysts with the total surface area 50–200 m² g⁻¹. Furthermore, for the photocatalytic reactions in solution (31), one needs to take into account the adsorption of the reactant on the surface of the photocatalyst. Adsorption of certain phenolic compounds obtained from lignocellulosic biomass has been reported, *e.g.* salicylic acid (33) in solution on TiO₂. With the rather high concentrations of isoeugenol and eugenol in solution used by us (0.5 M) and the high liquid/solid ratio as above, one should expect that the amount of adsorbed phenolic compounds will be insignificant *vs* the total amount present.

We have determined the molar concentration of the DHDIE product in the photocatalytic oxidation of isoeugenol in the presence of TiO₂ using the HPLC-UV-MS method. In the reference experiments conducted in the dark in the presence of TiO₂, no reaction products have been detected. Figure 7a shows the molar concentration of DHDIE obtained in the presence of TiO₂ *vs* dipole moment of the nonprotic solvents used.

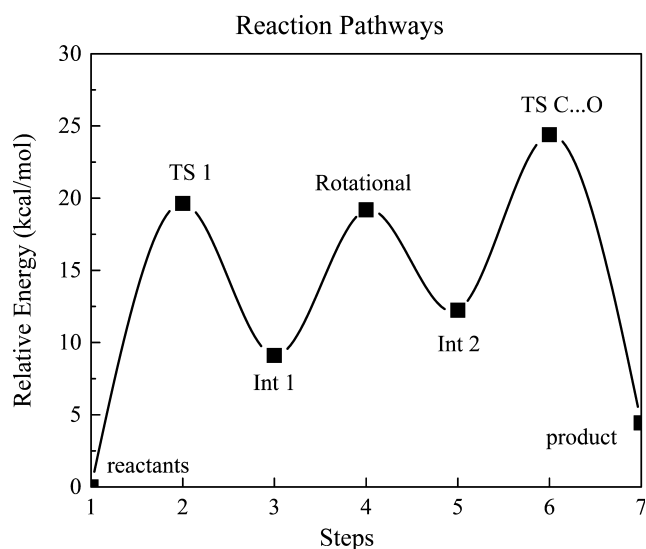


Figure 6. Reaction profile of the stepwise reaction of the radical of isoeugenol with the molecule of isoeugenol determined by the density functional theory (DFT) calculations.

Table 1. Total energies and energies relative to the van der Waals complex of the reactants. Energetically unfavorable TS2 (compared to TSr) is shown in italic font.

Structure	Total energy, Hartree	Energy vs the van der Waals complex of reactants, kcal mol ⁻¹
Reactants	-1075.582	0.0
TS1	-1075.550	19.6
Int1	-1075.567	9.1
TSr	-1075.551	19.2
Int2	-1075.562	12.2
TS CO	-1075.543	24.4
Products	-1075.574	4.4
TS2	<i>-1075.547</i>	<i>21.8</i>

One can see that the dependence is significantly different from that for the photochemical oxidation, compare Figs 5a and 7a. This indicates that there is some other factor that affects the yield of the DHDIE in the photocatalytic oxidation. Figure 7b shows the molar concentration of DHDIE obtained in the presence of TiO₂ vs the solubility of oxygen in each solvent. The solvents with the higher oxygen solubility (DMF and CH₃CN) show the higher yield of DHDIE that indicates the involvement of reactive oxygen species (ROS) in the photocatalytic oxidation of isoeugenol. Phenolic compounds from lignin containing olefinic C=C bond were reported to react with singlet oxygen in nonprotic solvents forming products from [2 + 4] cycloaddition reactions (endoperoxides) as well as from [2 + 2] cycloaddition reaction (54). Some of resultant peroxides have decomposed to yield the final anisaldehyde product, *i.e.* olefinic C=C bond in the reactant has been oxidized to aldehyde group (54). Singlet oxygen is known to be very strong nonselective oxidant; formation of singlet oxygen in significant amounts under our experimental conditions would have resulted in the products of oxidation of C=C bond in eugenol which did not form any products with or without titanium dioxide photocatalyst. Therefore, formation of singlet oxygen as reactive intermediate is unlikely under our experimental conditions; to definitely answer this question, a separate mechanistic study would be needed.

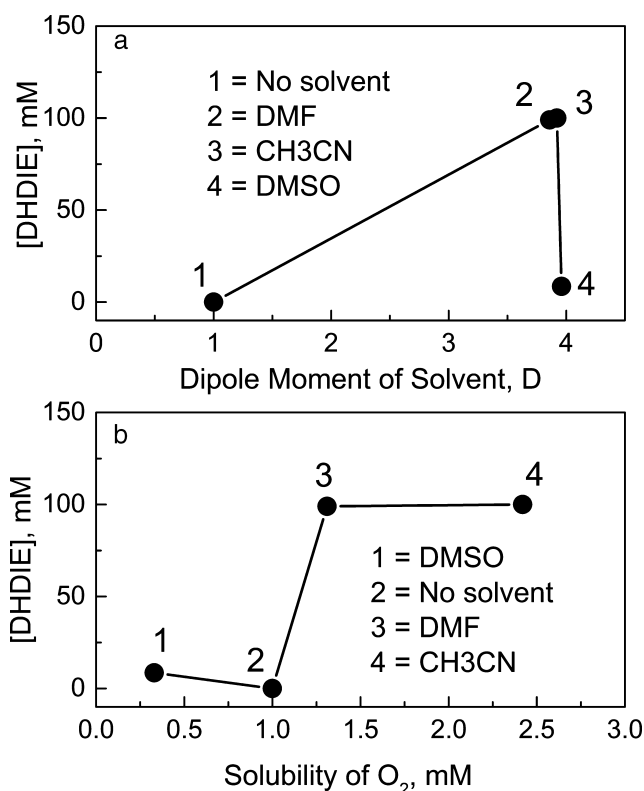
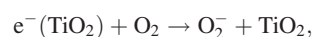
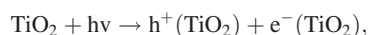


Figure 7. Molar concentration of the dehydrodiisoeugenol (DHDIE) product in the photocatalytic oxidation in solution: (a) vs the dipole moment of the solvent; (b) vs oxygen solubility in the solvent.

It is known that with water as solvent, a major ROS in the photocatalytic oxidation of organic compounds (55) is hydroxyl radical HO[•]. This hydroxyl radical is produced from water *via* its oxidation by the hole h⁺ formed in the valence band upon the photoexcitation of TiO₂. Hydroxyl radicals formed in illuminated aqueous suspensions of TiO₂ were detected by the electron paramagnetic resonance (EPR) spectroscopy with spin trapping method (56). Specifically, illumination at λ > 300 nm of aqueous suspension of TiO₂ with dissolved spin trap 5,5-dimethyl-1-pyrroline N-oxide (DMPO) resulted in the DMPO-OH[•] spin adduct *via* the interaction of hydroxyl radicals with DMPO. On the other hand, in the polar *nonprotic* solvents, a major ROS is the superoxide anion-radical O₂^{-•} as we noted in the recent review (31). In the nonprotic solvents, the anion-radical O₂^{-•} is formed by reduction of dissolved oxygen with electrons (57) generated in the conduction band of the photoexcited photocatalyst as follows, where *D* is the molecule of the substrate:



Anion-radicals O₂^{-•} were detected in the suspension of TiO₂ in acetonitrile under the illumination at 370 nm in the presence of oxygen by the EPR spectroscopy with DMPO spin trap (58). Interestingly, without solvent, isoeugenol produces only the small amounts of DHDIE in the photocatalytic oxidation (Fig. 7) which possibly indicates that the (polar) solvent stabilizes the

charged ROS. We propose that the selective photocatalytic oxidation of isoeugenol to DHDIE in acetonitrile (and possibly in DMF) proceeds *via* anion-radicals O_2^- ; experimental and computational work is in progress to test this hypothesis.

CONCLUSION

Selective activation of chemical bonds in sustainable phenolic compounds from plant biomass using light is important for producing “green” chemicals. For the first time, we report a selective activation of the C=C bond in isoeugenol *vs* isomeric eugenol by photocatalytic and photochemical oxidation to yield the lignan DHDIE. Selective photocatalytic oxidation with TiO_2 in the nonprotic solvents toward DHDIE reported here is drastically different from a well-known photocatalytic “complete mineralization” of phenolic compounds to carbon dioxide and water. Photooxidation in the nonprotic solvents also has the following advantages *vs* previously reported “mild” chemical oxidation: 1) photooxidation proceeds *via* an internal C=C bond, rather than *via* methoxy group or benzene ring, but not *via* a terminal C=C bond and 2) photooxidation leads to the fewer number of products than “mild” chemical oxidation. Results of this study can be used in development of “green” photochemical and photocatalytic selective synthesis of valuable chemicals from sustainable platform phenolic compounds of lignin origin; this will be addressed in future studies. For the first time, the stage-wise mechanism of oxidation of isoeugenol to DHDIE is proposed based on the DFT calculations.

Acknowledgements—A.S. sincerely thanks Rutgers University for his Research Council Grant 202221. The DFT calculations were performed using computer cluster of the Center for Computational and Integrative Biology (CCIB) of Rutgers University Camden.

SUPPORTING INFORMATION

Additional Supporting Information may be found in the online version of this article:

Figure S1. The DFT-optimized structure for reaction of isoeugenol radical with the molecule of isoeugenol: reactants. Green atoms: carbon; red atoms: oxygen; white atoms: hydrogen.

Figure S2. The DFT-optimized structure for reaction of isoeugenol radical with the molecule of isoeugenol: transition state Int1. Green atoms: carbon; red atoms: oxygen; white atoms: hydrogen.

Figure S3. The DFT-optimized structure for reaction of isoeugenol radical with the molecule of isoeugenol: transition state TSr. Green atoms: carbon; red atoms: oxygen; white atoms: hydrogen.

Figure S4. The DFT-optimized structure for reaction of isoeugenol radical with the molecule of isoeugenol: transition state Int2. Green atoms: carbon; red atoms: oxygen; white atoms: hydrogen.

Figure S5. The DFT-optimized structure for reaction of isoeugenol radical with the molecule of isoeugenol: transition state TS CO. Green atoms: carbon; red atoms: oxygen; white atoms: hydrogen.

Figure S6. The DFT-optimized structure for reaction of isoeugenol radical with the molecule of isoeugenol: DHDIE product. Green atoms: carbon; red atoms: oxygen; white atoms: hydrogen.

Figure S7. The DFT-optimized structure for reaction of isoeugenol radical with the molecule of isoeugenol: transition state TS2. Green atoms: carbon; red atoms: oxygen; white atoms: hydrogen.

Table S1. The Cartesian Coordinates in Angstroms and Gaussian input files for Reactants, TS1, Int1, TSr, Int2, TS CO, Products and intermediate TS2.

REFERENCES

- Corma, A., S. Iborra and A. Velty (2007) Chemical routes for the transformation of biomass into chemicals. *Chem. Rev.* **107**, 2411–2502.
- Chheda, J. N., G. W. Huber and J. A. Dumesic (2007) Liquid-phase catalytic processing of biomass-derived oxygenated hydrocarbons to fuels and chemicals. *Angew. Chem. Int. Ed.* **46**, 7164–7183.
- Zakzeski, J., P. C. A. Bruijninx, A. L. Jongerijs and B. M. Weckhuysen (2010) The catalytic valorization of lignin for the production of renewable chemicals. *Chem. Rev.* **110**, 3552–3599.
- Bortolato, S. A., K. E. Thomas, K. McDonough, R. W. Gurney and D. M. Martino (2012) Evaluation of photo-induced crosslinking of thymine polymers using FT-IR spectroscopy and chemometric analysis. *Polymer* **53**, 5285–5294.
- Trakhtenberg, S., R. Kumar, J. Bianchini, S. Thor, D. M. Martino and J. C. Warner (2007) Influence of pH and salt on the photocrosslinking in polyelectrolyte thymine-containing films. *J. Macromol. Sci., Pure Appl. Chem.* **44**, 1311–1315.
- Bortolato, S. A., K. McDonough, R. W. Gurney and D. M. Martino (2014) Second order multivariate curve resolution of Fourier transform infrared spectroscopic data of the photo-induced crosslinking of thymine functionalized polymers. *Talanta* **127**, 204–210.
- Fernando, S., S. Adhikari, C. Chandrapal and N. Murali (2006) Biorefineries: Current status, challenges, and future direction. *Energy Fuels* **20**, 1727–1737.
- Hatakeyama, H. and T. Hatakeyama (2010) Lignin structure, properties, and applications. In *Biopolymers: Lignin, Proteins, Bioactive Nanocomposites*, Vol. **232** (Edited by A. Abe, K. Dusek and S. Kobayashi), pp. 1–63. Springer-Verlag Berlin, Berlin.
- Melin, K. and M. Hurme (2010) Evaluation of lignocellulosic biomass upgrading routes to fuels and chemicals. *Cell. Chem. Technol.* **44**, 117–137.
- Sannigrahi, P., Y. Q. Pu and A. Ragauskas (2010) Cellulosic biorefineries—unleashing lignin opportunities. *Curr. Opin. Environ. Sustain.* **2**, 383–393.
- Parashuram, M. (2009) Kinetics and mechanisms of oxidation of 4-hydroxy-3-methoxy benzaldehyde (vanillin) by $Bi(V)$ in aqueous alkaline medium. *Int. J. PharmTech. Res.* **1**, 1234–1240.
- Sachdev, D., A. Dubey, B. G. Mishra and S. Kannan (2008) Environmentally benign liquid phase oxidation of vanillin over copper containing ternary hydrotalcites. *Catal. Commun.* **9**, 391–394.
- Elgendy, E. and S. Khayyat (2008) Oxidation reactions of some natural volatile aromatic compounds: Anethole and eugenol. *Russ. J. Org. Chem.* **44**, 823–829.
- Qamar, M. and M. Muneer (2009) A comparative photocatalytic activity of titanium dioxide and zinc oxide by investigating the degradation of vanillin. *Desalination* **249**, 535–540.
- Herrmann, W. A., T. Weskamp, J. P. Zoller and R. W. Fischer (2000) Methyltrioxorhenium: Oxidative cleavage of CC-double bonds and its application in a highly efficient synthesis of vanillin from biological waste. *J. Mol. Catal. A: Chem.* **153**, 49–52.
- Tang, S. L. Y., R. L. Smith and M. Poliakoff (2005) Principles of green chemistry: PRODUCTIVELY. *Green Chem.* **7**, 761–762.
- Montagnon, T., M. Tofi and G. Vassilikogiannakis (2008) Using singlet oxygen to synthesize polyoxygenated natural products from furans. *Acc. Chem. Res.* **41**, 1001–1011.
- Kuo, Y. H., L. H. Chen and L. M. Wang (1991) Photosensitized oxidation of isoeugenol in protic and aprotic-solvents. *Chem. Pharm. Bull.* **39**, 2196–2200.
- Davin, L. B., M. Jourdes, A. M. Patten, K.-W. Kim, D. G. Vassao and N. G. Lewis (2008) Dissection of lignin macromolecular configuration and assembly: Comparison to related biochemical processes

- in allyl/propenyl phenol and lignan biosynthesis. *Nat. Prod. Rep.* **25**, 1015–1090.
20. Ionescu, F., S. D. Jolad and J. R. Cole (1977) Dehydrodiisoeugenol: A naturally occurring lignan from *Aristolochia taliscana* (Aristolochiaceae). *J. Pharm. Sci.* **66**, 1489–1490.
 21. Li, F. and X.-W. Yang (2012) Analysis of anti-inflammatory dehydrodiisoeugenol and metabolites excreted in rat feces and urine using HPLC-UV. *Biomed. Chromatogr.* **26**, 703–707.
 22. Murakami, Y., S. Ito, T. Atsumi and S. Fujisawa (2005) Theoretical prediction of the relationship between phenol function and COX-2/AP-1 inhibition for ferulic acid-related compounds. *In Vivo* **19**, 1039–1043.
 23. Boyd, G. R., H. Reemtsma, D. A. Grimm and S. Mitra (2003) Pharmaceuticals and personal care products (PPCPs) in surface and treated waters of Louisiana, USA and Ontario, Canada. *Sci. Total Environ.* **311**, 135–149.
 24. Tixier, C., H. P. Singer, S. Oellers and S. R. Muller (2003) Occurrence and fate of carbamazepine, clofibrac acid, diclofenac, ibuprofen, ketoprofen, and naproxen in surface waters. *Environ. Sci. Technol.* **37**, 1061–1068.
 25. Teske, S. S. and R. G. Arnold (2008) Removal of natural and xenosterogens during conventional wastewater treatment. *Rev. Environ. Sci. Biotechnol.* **7**, 107–124.
 26. Chen, X. P., S. S. Xu, T. F. Tan, S. T. Lee, S. H. Cheng, F. W. F. Lee, S. J. L. Xu and K. C. Ho (2014) Toxicity and estrogenic endocrine disrupting activity of phthalates and their mixtures. *Int. J. Environ. Res. Public Health* **11**, 3156–3168.
 27. Eskins, K., C. Glass, W. Rohrwedder, R. Kleiman and J. Sloneker (1972) Dimers of isoeugenol by dye-sensitized photooxidation. *Tetrahedron Lett.* **9**, 861–864.
 28. DellaGreca, M., M. R. Iesce, L. Previtiera, R. Purcaro, M. Rubino and A. Zarrelli (2008) Lignans by photo-oxidation of propenyl phenols. *Photochem. Photobiol. Sci.* **7**, 28–32.
 29. Birney, D. M. (2010) Theory, experiment and unusual features of potential energy surfaces of pericyclic and pseudopericyclic reactions with sequential transition structures. *Curr. Org. Chem.* **14**, 1658–1668.
 30. Bakalbassis, E. G., N. Nenadis and M. Tsimidou (2003) A density functional theory study of structure-activity relationships in caffeic and dihydrocaffeic acids and related monophenols. *J. Am. Oil Chem. Soc.* **80**, 459–466.
 31. Samokhvalov, A. (2011) Heterogeneous photocatalytic reactions of sulfur aromatic compounds. *ChemPhysChem* **12**, 2870–2885.
 32. Rao, C. R. N., T. Takashima, W. A. Bradley and T. Y. Lee (1984) Near ultraviolet radiation at the earth's surface: Measurements and model comparisons. *Tellus. B* **36B**, 286–293.
 33. Johnson, A. M., S. Trakhtenberg, A. S. Cannon and J. C. Warner (2007) Effect of pH on the viscosity of titanium dioxide aqueous dispersions with carboxylic acids. *J. Phys. Chem. A* **111**, 8139–8146.
 34. Amat, A. M., A. Arques, F. López and M. A. Miranda (2005) Solar photo-catalysis to remove paper mill wastewater pollutants. *Sol. Energy* **79**, 393–401.
 35. Taylor, S., M. Mehta and A. Samokhvalov (2014) Production of hydrogen by glycerol photoreforming using binary nitrogen-metal-promoted N-M-TiO₂ photocatalysts. *ChemPhysChem* **15**, 942–949.
 36. Samokhvalov, A., S. Nair, E. C. Duin and B. J. Tatarchuk (2010) Surface characterization of Ag/titania adsorbents. *Appl. Surf. Sci.* **256**, 3647–3652.
 37. McDow, S. R., Q. R. Sun, M. Vartiainen, Y. S. Hong, Y. L. Yao, T. Fister, R. Q. Yao and R. M. Kamens (1994) Effect of composition and state of organic-components on polycyclic aromatic hydrocarbon decay in atmospheric aerosols. *Environ. Sci. Technol.* **28**, 2147–2153.
 38. Gerasimov, A. V., N. V. Gornova and N. V. Rudometova (2003) Determination of vanillin and ethylvanillin in vanilla flavorings by planar (thin-layer) chromatography. *J. Anal. Chem.* **58**, 677–684.
 39. Leopold, B. (1950) Aromatic keto- and hydroxy-polyethers as lignin models. III. *Acta Chem. Scand.* **4**, 1523–1537.
 40. Bortolomeazzi, R., G. Verardo, A. Liessi and A. Callea (2010) Formation of dehydrodiisoeugenol and dehydrodieugenol from the reaction of isoeugenol and eugenol with DPPH radical and their role in the radical scavenging activity. *Food Chem.* **118**, 256–265.
 41. Frisch, M. J., G. W. Trucks, H. B. Schlegel, G. E. Scuseria, M. A. Robb, J. R. Cheeseman, G. Scalmani, V. Barone, B. Men-
nucci, G. A. Petersson, H. Nakatsuji, M. Caricato, X. Li, H. P. Hratchian, A. F. Izmaylov, J. Bloino, G. Zheng, J. L. Sonnenberg, M. Hada, M. Ehara, K. Toyota, R. Fukuda, J. Hasegawa, M. Ishida, T. Nakajima, Y. Honda, O. Kitao, H. Nakai, T. Vreven, J. J. A. Montgomery, J. E. Peralta, F. Ogliaro, M. Bearpark, J. J. Heyd, E. Brothers, K. N. Kudin, V. N. Staroverov, R. Kobayashi, J. Normand, K. Raghavachari, A. Rendell, J. C. Burant, S. S. Iyengar, J. Tomasi, M. Cossi, N. Rega, J. M. Millam, M. Klene, J. E. Knox, J. B. Cross, V. Bakken, C. Adamo, J. Jaramillo, R. Gomperts, R. E. Stratmann, O. Yazyev, A. J. Austin, R. Cammi, C. Pomelli, J. W. Ochterski, R. L. Martin, K. Morokuma, V. G. Zakrzewski, G. A. Voth, P. Salvador, J. J. Dannenberg, S. Dapprich, A. D. Daniels, Ö. Farkas, J. B. Foresman, J. V. Ortiz, J. Cioslowski and D. J. Fox (2009) *Gaussian 09 Revision D. 01*. Wallingford, CT.
 42. Adamo, C. and V. Barone (1999) Toward reliable density functional methods without adjustable parameters: The PBE0 model. *J. Chem. Phys.* **110**, 6158–6170.
 43. Ernzerhof, M. and G. E. Scuseria (1999) Assessment of the Perdew–Burke–Ernzerhof exchange–correlation functional. *J. Chem. Phys.* **110**, 5029–5036.
 44. Franco, C. and J. Olmsted (1990) Photochemical determination of the solubility of oxygen in various media. *Talanta* **37**, 905–909.
 45. Alfonsi, K., J. Colberg, P. Dunn, T. Fevig, S. Jennings, T. Johnson, H. Kleine, C. Knight, M. Nagy, D. Perry and M. Stefaniak (2008) Green chemistry tools to influence a medicinal chemistry and research chemistry based organisation. *Green Chem.* **10**, 31–36.
 46. Martin, D., A. Weise and H.-J. Niclas (1967) The solvent dimethyl sulfoxide. *Angew. Chem. Int. Ed.* **6**, 318–384.
 47. de Jager, L. S., G. A. Perfetti and G. W. Diachenko (2007) Determination of coumarin, vanillin, and ethyl vanillin in vanilla extract products: Liquid chromatography mass spectrometry method development and validation studies. *J. Chromatogr. A* **1145**, 83–88.
 48. Battino, R., T. R. Rettich and T. Tominaga (1983) The solubility of oxygen and ozone in liquids. *J. Phys. Chem. Ref. Data* **12**, 163–178.
 49. Rodriguez-Evora, Y. and N. P. Schepp (2005) Reactivity of 4-vinylphenol radical cations in solution: Implications for the biosynthesis of lignans. *Org. Biomol. Chem.* **3**, 4444–4449.
 50. Adamo, C. and D. Jacquemin (2013) The calculations of excited-state properties with Time-Dependent Density Functional Theory. *Chem. Soc. Rev.* **42**, 845–856.
 51. Lan, Y., L. Zou, Y. Cao and K. N. Houk (2011) Computational methods to calculate accurate activation and reaction energies of 1,3-dipolar cycloadditions of 24 1,3-dipoles. *J. Phys. Chem. A* **115**, 13906–13920.
 52. Ohtani, B., O. O. Prieto-Mahaney, D. Li and R. Abe (2010) What is Degussa (Evonik) P25? Crystalline composition analysis, reconstruction from isolated pure particles and photocatalytic activity test. *J. Photochem. Photobiol. A Chem.* **216**, 179–182.
 53. Kisch, H. (2010) On the problem of comparing rates or apparent quantum yields in heterogeneous photocatalysis. *Angew. Chem. Int. Ed.* **49**, 9588–9589.
 54. Greer, A., G. Vassilikogiannakis, K.-C. Lee, T. S. Koffas, K. Nahm and C. S. Foote (2000) Reaction of singlet oxygen with trans-4-propenylanisole. Formation of [2 + 2] products with added acid. *J. Org. Chem.* **65**, 6876–6878.
 55. Pelaez, M., N. T. Nolan, S. C. Pillai, M. K. Seery, P. Falaras, A. G. Kontos, P. S. M. Dunlop, J. W. J. Hamilton, J. A. Byrne, K. O'Shea, M. H. Entezari and D. D. Dionysiou (2012) A review on the visible light active titanium dioxide photocatalysts for environmental applications. *Appl. Catal. B-Environ.* **125**, 331–349.
 56. Brezova, V., D. Dvoranova and A. Stasko (2007) Characterization of titanium dioxide photoactivity following the formation of radicals by EPR spectroscopy. *Res. Chem. Intermed.* **33**, 251–268.
 57. Sawyer, D. T., G. Chiericato, C. T. Angelis, E. J. Nanni and T. Tsuchiya (1982) Effects of media and electrode materials on the electrochemical reduction of dioxygen. *Anal. Chem.* **54**, 1720–1724.
 58. Noda, H., K. Oikawa, H. Ohyanishiguchi and H. Kamada (1993) Detection of superoxide ions from photoexcited semiconductors in nonaqueous solvents using the ESR spin-trapping technique. *Bull. Chem. Soc. Jpn.* **66**, 3542–3547.